USE OF MAPS IN THE EXPLORATION OF ELECTRON CLOUD PARAMETER SPACE

U. Iriso*, and S. Peggs.
BNL, Upton, NY 11973, USA

Abstract

The optimal distribution of the bunch pattern around the RHIC circumference is studied to decrease the electron density for a fixed total beam current. In the search for a bunch pattern that minimizes this density, we show that, for typical parameters, the bunch-to-bunch evolution of the electron cloud density can be represented by a cubic map. Furthermore, we discuss the use of linear bunch-to-bunch maps for small electron cloud densities. The linear coefficients evaluate the electron cloud stability for a given set of physical parameters (bunch charge, SEY, et cetera). Thus, the use of (linearized) maps frees up the slow but detailed simulation codes to explore parameter space, when studying the increase (to a saturated value) or disappearance of the electron cloud under alternative bunch patterns.

MOTIVATION

Electric fields present in many vacuum systems may accelerate electrons (produced by field emission, photoemission, ionization of residual gas ionization, et cetera) towards the wall chamber surface. If the bombarding electrons acquire enough energy, they produce secondary electrons, which in turn may be accelerated if the electric field normal to the surface is in the correct phase. These electrons may bombard another surface and emit again secondary electrons. This bouncing back and forth between surface is the electron *multipacting* effect. This name is derived from "resonance of multiple electron impact", and it was first described by Farnswoth in 1934 [1]. If the number of emitted electrons per impinging electron, given by the Secondary Emission Yield (SEY) of the wall surface, is greater than unity, the electron density inside the pipe increases (initially) exponentially, creating a so-called Electron Cloud (EC). This EC can eventually lead to the development of vacuum breakdown and other system failures.

Since 1965, when a coherent betatron oscillation and beam loss in presence of bunched beams were observed in BINP in Novosibirsk [2], footprints of electron multipacting produced by the beam electric field have been detected in many accelerators. In 1972, the ISR at CERN showed excitation of nonlinear resonances and gradual beam blow up in presence of proton coasting beams, with a beam induced signal from a pick up showing coupled electron-proton oscillations [3]. After a couple of decades, electron driven instabilities started to be an issue in several machines (see Reference [4] for an historical overview on Electron Cloud effects), and finally, in 1997 CERN launched a crash program to study the effects of the Electron Cloud due to its important impact on the LHC.

Several computer codes have been successfully developed and benchmarked with experimental observations since the late nineties to study the build up conditions of this effect. A comparison among the different codes was made [5] after the "ECLOUD Workshop02" held in Geneva in 2002 [6]. Typically, these codes work either by Particle In Cell methods (like CLOUDLAND [7]), or by tracking the electrons grouped in macro-particles, where each macro-particle can join up to a maximum of around 10^5 electrons (like ECLOUD [8], or CSEC [9]). In the latter case, when a macro-particle produces more electrons, the total Coulomb charge of this macro-particle is increased. At every time step, these detailed codes compute the necessary physical forces/fields influencing the motion of the macro-particles. If EC formation takes place, the total number of electrons is about 10^{10} (depending on the parameters for every case), hence the need to group the electrons in macro-particles. These codes use a considerable amount of CPU time: a complete EC simulation, depending specially on the simulation parameters, can last from around 1 hour to some days. In the cases we studied here (for the parameters seen in Table 1), a single simulation last about 1 hour.

THE BUNCH TO BUNCH EVOLUTION

In case of a multi-bunch electron cloud, where the electric field accelerating the electrons is given by a bunched beam, it is postulated that the evolution of the electron cloud density can be followed using logistic maps. This frees up the detailed simulation codes and enhances physical intuition through the use of standard maths. For a given beam pipe characteristics (SEY, chamber dimensions, etc), the evolution of the electron density, ρ, is only driven by the bunch m passing by, and the existing electron density before the bunch passed by. Following the logistic map formalism, this would be expressed as:

$$\rho_{m+1} = \alpha\, \rho_m (1 - \rho_m) \quad , \tag{1}$$

and the parameter α would be a first function of the beam parameters, such as bunch intensity, N; bunch spacing, s_b; bunch length, σ_z; and bunch transverse size, r_b. Ultimately, α would be a function of the beam pipe characteristics: maximum SEY, $\delta_{\max}$; electron energy at which SEY is maximum, $E_{\max}$; reflectivity at zero electron energy, δ_0;

* ubaldo@bnl.gov

beam pipe dimensions, etc:

$$\alpha = \alpha(N, s_b, \sigma_z, r_b, ... \; ; \; \delta_{\max}, E_{\max}, R_0, ...) \quad . \qquad (2)$$

Therefore, α would be a mathematical tool concentrating the EC dependence of the physical parameters. This formalism evidences one of the main known characteristics of the electron cloud, the initial exponential growth [13]:

$$\rho \approx \rho_0 \, e^{m(\alpha-1)} \quad , \qquad (3)$$

is now explained with Eq. 1. From the latter expression, the saturated electron cloud density, $\rho_{\rm sat}$ is determined simply by:

$$\rho_{\rm sat} = 0 \qquad N < N_C \qquad (4)$$

$$\rho_{\rm sat} = \frac{\alpha - 1}{\alpha} \qquad N > N_C \qquad (5)$$

showing a phase transition from electron cloud "off" to "on". If α increases smoothly with N, the phase transition is second order. However, RHIC data shows both first and second order electron cloud phase transitions [14]. Note that the units in Eq. 1 do not fit, and requires ρ_m to be unitless. Equation 1 is only a mathematical tool to express our purposes. Although the logistic map formalism is finally not appropriate, it illustrates the goal of this study: simplify the EC problem into a small number of mathematical parameters. In the example of the logistic maps, the sole parameter is α.

We then tackle the problem by testing if the existing computer simulations confirm that the electron cloud evolution can be represented by maps. For this purpose, we center the following studies on the RHIC case. Table 1 shows the physical parameters used for these simulations. Besides the beam characteristics, the SEY behavior as a function of the impinging electron energy is a key parameter in the electron cloud development. All simulation codes are strongly dependent of the model used for the SEY behavior [10]. In this case, CSEC uses the model by M. Furman and M. Pivi described in [11], where one can find detailed explanations of the parameters named in the second part of Table 1. On the other hand, ECLOUD uses the model described in [10]. Table 1 compares only the most "common" surface physics parameters. It is worth mentioning that whereas ECLOUD uses a Gaussian distribution for the emitted secondary electrons, CSEC uses a Lorentzian one (parameter $\sigma_{\rm sec}$ in Table 1).

Note that with this bunch spacing and given the RHIC revolution period, we can inject up to 120 bunches (not counting the limitations given by the abort gap kickers, which would decrease this number to 110). Nevertheless, for the purpose of this study we are interested in the build up and decay evolution of the electron density. Therefore, launching the simulation until the saturation is reached, (which is well achieved after 60 consecutive bunches) minimizes the CPU time.

A typical time evolution of the electron density has a similar pattern to what is shown in Fig. 1. This corresponds to the case of injecting 60 bunches with 1.4×10^{11} protons in the ring spaced by the minimum RHIC bunch spacing (108 ns). The electron density per beam pipe meter, ρ, as a function of time grows (initially) exponentially until the space charge due to the electrons themselves produces a saturation level. Once the saturation level is reached the average electron density does not change significantly. In this case, the code used is CSEC (Cylindrical Symmetric Electron Cloud simulation) [12]. The red line shows CSEC output, while the grey circles mark the average electron density between the passage of two bunches, no matter if they are full bunches or empty. Obviously, in the bunch to bunch evolution, the time step is now integer multiples of the bunch spacing. In Fig. 1 one can see that following the evolution "bunch-to-bunch" does not produce a lack of information about the build-up or the decay time, although the details of the electron density oscillation between two bunches are lost.

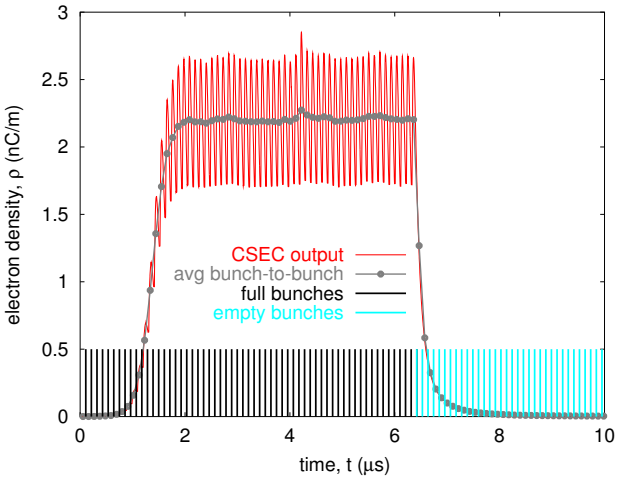

Figure 1: Time evolution of the electron density (red line) computed with CSEC during 10 μs a (RHIC time revolution is 12.82 μs). The case corresponds to the injection of 60 successive bunches with a bunch spacing of 108 ns and a bunch intensity of $N = 1.4 \times 10^{11}$ protons (marked with black bars), followed by 60 "empty" bunches (marked with light blue bars). The grey circles mark the average electron density between two consecutive bunches.

THE CUBIC MAP

Using the parameters shown in Table 1, the bunch to bunch evolution of the electron cloud density is followed averaging the output of two codes, CSEC and ECLOUD, for different bunch intensities, N, from 6×10^{10} to 2×10^{11} protons, in steps of $\Delta N = 2 \times 10^{10}$ protons. Figure 2 shows how the electron density after the bunch m passes by, ρ_{m+1}, behaves as a function of the previous electron density, ρ_m, for different bunch intensities, N. The points in Fig. 2 show the average electron cloud density between two bunches using results from CSEC (Fig. 2, left) and

Table 1: List of input parameters for electron cloud simulations. In all cases, the simulations using CSEC and ECLOUD are performed for protons bunches.

			CSEC	ECLOUD
parameter	symbol	unit	value	value
bunch spacing	s_b	ns	108	108
# of bunches	M	...	60	60
beam radius	r_b	mm	2.4	2.4
full bunch length	σ_z	ns	18	21
protons/bunch	N	10^{10}	8 to 20	8 to 20
revolution time	$t_{\rm rev}$	μs	12.82	12.79
beam energy	E	GeV	27.7	11.46
beam pipe diameter	d	mm	120	120
reflectivity at zero energy	δ_0	...	0.6	1.0
reflectivity at infinite energy	P_∞	...	0.2	...
rediffusion probability	$P_{\rm rd}$	...	0.5	...
reflection energy	$E_{\rm rf}$	eV	60	60
maximum SEY	$\delta_{\rm max}$	...	2.3	2.3
energy for maximum SEY	$E_{\rm max}$	eV	310	310
energy for secondary e-	$E_{\rm sec}$	eV	8.9	7.0
energy width for secondary e-	$\sigma_{\rm sec}$	eV	4.5	5.5
initial e- density	$\rho_{\rm ce}$	pC/m	0.2	–
electrons generated/bunch	...	...	35000	–
electron generation radius	...	mm	60	–
# slices per bunch	...	...	60	100
# slices per inter-bunch	...	...	840	100
initial # of macro-particles	...	...	25	–
maximum # of macro-particles	...	...	10^5	$\approx 10^5$

ECLOUD (Fig. 2, right). The lines correspond to cubic fits with no constant term:

$$\rho_{m+1} = a\,\rho_m + b\,\rho_m^2 + c\,\rho_m^3 \quad . \tag{6}$$

Figure 2 is explained as follows: starting with a small initial linear electron density $\rho_0 \neq 0$ (due to beam-gas ionization, beam losses, etc), after some bunches the density takes off and reaches the corresponding saturation line ($\rho_{m+1} = \rho_m$, red trace) when the space charge effects due to the electrons of the cloud itself takes place. In this situation, all the points (corresponding to the passage of full bunches) are in the same spot. The justification of the three terms is explained as a consequence of the linear growth, a parabolic decay due to space charge effects, and a cubic term corresponding to perturbations (electrons generated by residual gas ionization, beam losses, etc).

The electron cloud decay is described as the succession of bunches with a null bunch intensity, $N = 0$. Neglecting the point corresponding to the electron cloud density after the first empty bunch, the electron density follows a similar decay independently of the initial value of the saturated electron density.

It is worth stressing the behavior of this "first empty" bunch, corresponding to the $N = 0$ bunches. The points coming from different saturation values, $\rho_{\rm sat}$ lye off on a general curve, which we call "first $N = 0$", or "first empty bunch" curve. This is explained as a consequence of the dominance of the space charge effects of the saturation. In other words, it takes two bunches to jump from a curve $N \neq 0$ to the decay ($N = 0$ curve).

Thus, for the parameters shown in Table 1, the electron density build up for a given bunch intensity is determined by a 3-dimensional vector $\vec{A}(N) = (a, b, c)$, while decay is described by two vectors, one corresponding to the "first ghost bunch", and a second vector for the rest of them. Figure 3 shows how the coefficients (a, b, c) evolve as a function of the bunch intensity, N, for both CSEC (grey points), and ECLOUD (red squares). Explanation of the physical meaning of these parameters follows. First, for this bunch spacing and surface parameters, both codes give a similar phase transition threshold, around 7×10^{10} protons. For $N > 8 \times 10^{10}$ protons, the linear coefficient, a, becomes larger than 1 for both ECLOUD and CSEC, and increases linearly in a first approximation. For large N, a grows more slowly because the space charge effects have a faster influence: the more bunch intensity, the more electrons are created after a bunch passage, and therefore the space charge effects will be sooner noticeable. This is equivalent to say that the build up time tends to stabilize with increasing bunch intensities.

In all cases (different N), and using both codes, the quadratic coefficient, b, is negative to give concavity to the electron cloud density evolution in the space (ρ_m, ρ_{m+1}). This coefficient decreases (increases in absolute value) for

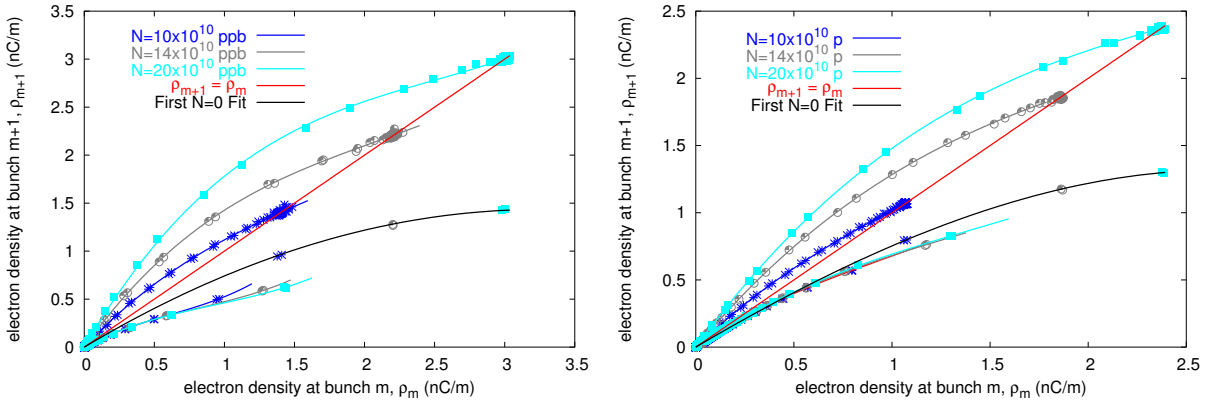

Figure 2: Average electron density after the bunch m passes by, ρ_{m+1}, as a function of the electron density before the bunch m passed by, ρ_m, for different bunch intensities, N. The left hand plot shows the CSEC output, while the points on the right hand plot come from ECLOUD simulation. In both cases, the lines correspond to cubic fits applied to the average bunch to bunch points.

CSEC results, showing that as increasing the bunch intensity, N, the space charge effects are gaining influence. However, using ECLOUD results, b only decreases for bunch intensities $N > 12 \times 10^{10}$ protons. It is surprising that b is not a monotonic function of the bunch intensity. The cubic coefficient, c, is associated with electrons created by other mechanisms than the electron multipacting. This term is positive, consistent with the expectations, and one order of magnitude smaller than the linear term for $N > 10^{10}$ protons. However, both codes differ significantly for $N < 10^{10}$ protons. The proximity to the bunch intensity threshold, and the different ways both codes compute other electron sources are associated with these difference.

The need for cubic terms is strong when large electron cloud densities are produced by large bunch intensities. Large electron cloud densities (not produced for the bunch intensities handled by RHIC) perhaps need higher order expressions. This fact suggests that the cubic map is the Taylor expansion of a more universal form, for example:

$$\rho_{m+1} = \frac{a' \cdot \rho_m}{1 + b' \cdot \rho_m} = a\,\rho_m + b\,\rho_m^2 + c\,\rho_m^3 + \ldots \quad . \quad (7)$$

It is found that maps such as this do not improve on the cubic map, therefore we continue the analysis using cubic maps.

MINIMIZATION OF ELECTRON DENSITY AT RHIC

After experimental observations during Run-3 [15, 16, 17], it was found that the use of gaps along the bunch train can be useful against the build up of the electron cloud. Since the growth time is longer than the decay time (see, for example, Fig. 1) the goal is to find out a bunch pattern around the RHIC circumference that does not trigger the electron cloud, or minimizes the detrimental effects of the phenomenon. In the following we will use triplets of integer numbers (k_s, k_b, k_g) to describe bunch patterns, where k_s gives the bunch spacing in buckets, k_b the number of bunches filled with that spacing, and k_g the number of "phantom" bunches added, i.e. bunches that are not filled in and therefore create a gap. Changing patterns can then be described by adding a new triplet. For example the configuration (2,2,1)(3,4,0) would correspond to the pattern

1-0-1-0-0-0-1-0-0-1-0-0-1-0-0-1-0-0

where 1 denotes a filled and 0 denotes an empty bucket. If not otherwise noted, it is assumed that a pattern repeats until the abort gap is reached. When using the 28 MHz RF cavities, RHIC has an harmonic number of 360 buckets, and it is allowed to inject a bunch every 3 buckets (minimum) with an abort gap of 30 buckets. In terms of possible bunches, this implies a maximum of 110 bunches.

In the following, different distributions of 68 bunches are discussed. Figure 4 shows the result of three attempts in injecting three different bunch patterns: (3,16,4), (3,12,8), and (3,14,6). Even though pressure rises are detected for the first two cases and not for the third one, (see pressure rise at the blue section in Fig. 4, bottom), we can inject up to 68 bunches using the configuration (3,12,8), whereas injection of bunch pattern (3,14,6) cannot be completed. A comparison among the three cases is complicated by the fact that bunch intensity and bunch length are not the same for all fills. Figure 4 also shows that the attempt to fill bunch pattern (3,14,6) was successful, but it is not taken into account for this study because the bunch length was the double of the previous attempted fills. Bunch intensity and length are comparable for fills (3,16,4) and (3,12,8), which also show similar vacuum behavior. On the other hand, fill (3,14,6) has bunch lengths that are larger by a factor of 2 compared to previous attempts. This, together with the

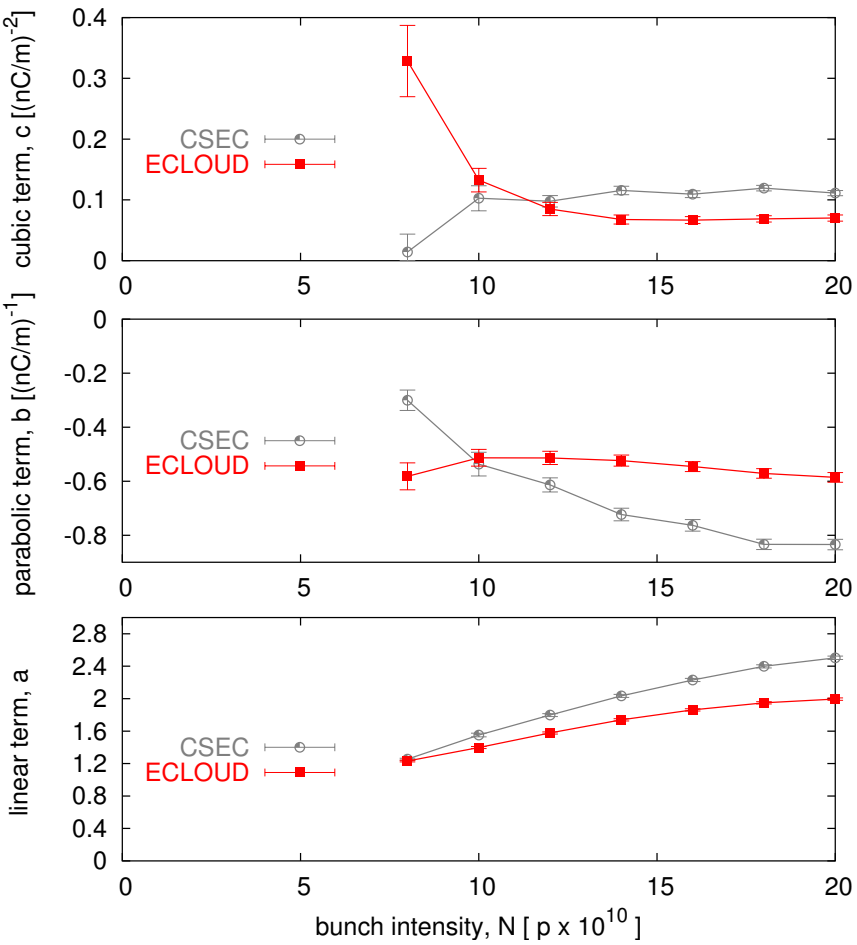

Figure 3: Evolution of the linear, a, parabolic, b, and cubic c terms determining the electron cloud build up as a function of the bunch intensity, N, for both ECLOUD (red squares) and CSEC (grey points).

reduced bunch intensity, can account for the suppression of ECs. Table 2 summarizes the characteristics of the different cases and compares the relative luminosity.

Reference [15] studies the effect of the bunch pattern on the EC and pressure rise. Several computer simulation runs were launched with different bunch patterns. The criteria to minimize the effects of the electron cloud were the comparison between the average and the maximum value of the electron density created by each bunch pattern. The conclusion, in agreement with the way B-factories work, is that the most sparse distribution of bunches is the best way to optimize luminosity. However, assuming that one CSEC run takes about 1 h, if we want to study all the possibilities of distributing 68 bunches in 110 possible buckets, it is obvious that we cannot simulate

$$\frac{110!}{(110-68)!\times 68!} \approx 10^{30}$$

different bunch distributions. In this section, we will show how maps elegantly answer the initial question: given a fixed beam intensity, what is the optimum bunch distribution along the bunch train to minimize the electron cloud density?

First $N_m = 0$ and $N_m = 1$

The bunch to bunch simulations carried out with CSEC and reported in [15] are reproduced and compared using MEC (Maps for Electron Cloud). The parameters used in all cases are shown in Table 1. The use of MEC is divided in four cases, depending on the bunch charge of the bunch m passing by:

- "Full" bunches, which in this case denote bunches with charge $N = 8 \times 10^{10}$ protons. The cubic form is similar to Eq. 6, and the coefficients are denoted using the vector $\vec{A}_{11} = (a_{11}, b_{11}, c_{11})$.
- "Empty" bunches, which denote bunches with bunch charge $N = 0$. In this case the corresponding cubic form is obtained from the decay case, and it is denoted with the vector $\vec{A}_{00} = (a_{00}, b_{00}, c_{00})$.
- First "empty" bunch, which denotes an empty bunch after a populated bunch, i.e. $N_m = 0$ and $N_{m-1} =$

Table 2: Comparison of bunch patterns tested in RHIC at injection.

parameter	unit	reference case	fill no 1	fill no 2	fill no 3
bunch pattern	...	(6,1,0)	(3,16,4)	(3,12,8)	(3,14,6)
no of bunches	...	56	41	69	78
average proton/bunch N	10^{11}	1.0	1.1	1.0	0.9
total intensity	10^{11}	56.0	44.3	68.1	70.2
full bunch length	ns	...	16.5	17.6	34.2
pressure rise	...	...	yes	yes	no
luminosity scaling factor	...	1.00	0.88	1.23	1.13

1. The corresponding cubic form is denoted with the vector: $\vec{A}_{01} = (a_{01}, b_{01}, c_{01})$.

- First "full" bunch, which denotes a full bunch after an empty one, i.e. $N_m = 1$ and $N_{m-1} = 0$. The corresponding cubic form is denoted with the vector: $\vec{A}_{10} = (a_{10}, b_{10}, c_{10})$.

The need of this subdivision requires analysis of two figures: in Fig. 2 one can see that the "first $N_m = 0$" is out of the evolution of decay curve, i.e. the curve corresponding to "phantom" bunches.

Figure 5 justifies the case for the "first $N_m = 1$" curve. Figure 5 evidences that the transition from "empty" to "full" also requires two bunches, in the same way that the transition from "full" bunch to "empty" bunch is done in two bunches. One obtains successful results when comparing the bunch to bunch evolution using CSEC and MEC: see the graphical comparison between the bunch to bunch evolution using the two codes at Figures 6, 7, 8, and 9. Table 3 compares numerically the maximum and average values for the linear electron cloud density at the last turn following the ns to ns evolution in [15], and the bunch to bunch evolution using CSEC and MEC. The largest difference is between a 15% for the maximum density (corresponding to the case (3,2,0)(6,4,0)), while for the average density the maximum difference is within an error bar of 17%, corresponding to the case (3,23,17). While CSEC uses about $\approx$ 1 h CPU time for each case, MEC is obviously much faster and only uses $\approx$ 1 ms, which represents a speed up of seven orders of magnitude.

The linear approximation

Four sets of polynomial coefficients, $\vec{A}_{11}(N)$, $\vec{A}_{01}(N)$, $\vec{A}_{00}(N)$, and $\vec{A}_{10}(N)$, are required to follow the bunch to bunch evolution of the electron cloud density. Figure 5 suggests that for small electron densities, its bunch to bunch evolution can be considered as linear in the (ρ_m, ρ_{m+1}) space. If there is a total number of M bunches in a ring with a "bunch harmonic" number of H, the linearization of the problem gives a one turn map that is simply:

$$\rho_{m+H} \;\approx\; F(N)\,\rho_m \tag{8}$$

where the "one turn factor"

$$F \;\equiv\; (a_{10}\,a_{01})^i\; a_{11}^{M-i}\; a_{00}^{H-M-i} \tag{9}$$

and i is the number of transitions from full to empty (and empty to full) bunches. In general the minimum possible number of transitions is $i = 1$ (if all the bunches are clumped together), and the maximum number of transitions is the smaller of M and $H - M$ (when the bunches are spread as sparsely as possible). The special case $i = 0$ applies when there is no abort gap, $M = H$.

It is clear that if $F > 1$ then the electron cloud density increases (to some saturated value), while if $F < 1$ then the cloud disappears. When the one turn factor is rewritten as

$$F \;=\; \left(\frac{a_{10}\,a_{01}}{a_{11}\,a_{00}}\right)^i \left(\frac{a_{11}}{a_{00}}\right)^M a_{00}^H \tag{10}$$

it is clear that, for given M and H and N, the smallest (largest) value of F occurs for the largest (smallest) allowed value of i if

$$\left(\frac{a_{10}\,a_{01}}{a_{11}\,a_{00}}\right) \;<\; 1 \tag{11}$$

and vice versa. Since Eq. 11 is valid for RHIC parameters, which shows that either the most sparse distribution of a fixed number of fixed population bunches is the most stable against electron cloud growth.

Thus, from the mapping approach and using standard maths we analytically demonstrate that the most sparse distribution of bunches in a ring circumference minimizes the detrimental effects of the multi-bunch electron cloud effects. This is not a big surprise if we consider the possibility of evenly distributed bunches, i.e. the same bunch spacing between all bunches. In this case, the most sparse distribution of bunches is equivalent to use the larger bunch spacing between them. However, Eq. 10 demonstrates that this idea is also valid for unevenly spaced bunches along a bunch train.

ELECTRON CLOUD PHASE TRANSITION

We introduced in earlier sections the question how do electron clouds go through the transition "on" to "off". The

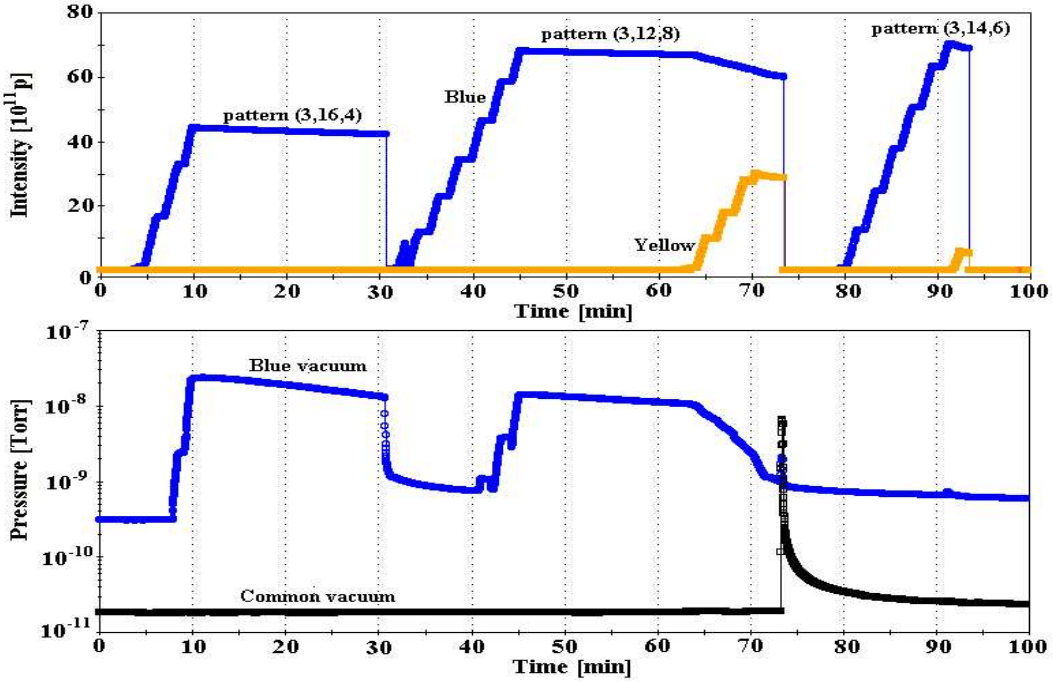

Figure 4: Attempt of filling RHIC with three different bunch patterns: (3,16,4), (3,12,8), and (3,14,6). The top plot shows the total intensity in the ring, while the bottom plot shows the pressure in one of the unbaked warm regions at RHIC (blue vacuum). Unlike the first attempt, (3,16,4), the injection in the second case, (3,12,8), does not prevent machine operation although the pressure rise is noticeable. The third case, (3,14,6) is not taken into account due to an unusually large bunch spacing.

exploration of parameter space should en-light this process, as claimed already in [18], where the analogy of electron cloud effects and ferromagnetic phases are announced. This is not a big surprise, phase transitions are present in many physical systems, from the above mentioned ferromagnetic example to the more known thermodynamics systems, or even the vehicle flow traffic versus the density of vehicles show a first order phase transitions [19].

In the case of electron cloud density, it is reasonable to expect on general grounds that

$$\rho = 0 \qquad N < N_C \qquad (12)$$

$$\rho \approx \kappa\,(N - N_C)^{\beta} \qquad N > N_C \qquad (13)$$

where the coefficients κ and β depend on the details of the physics, and N_c marks the bunch intensity threshold that triggers the electron cloud. The approximation 13 is valid for values of N in the vicinity of N_c. Now add the assumption that the bunch population decays at an approximately constant smooth rate dN/dt near the time T_C at which it crosses the critical population N_C, so that

$$N \approx N_C + \frac{dN}{dt}(t - T_C) \qquad (14)$$

In this case the decay of the electron cloud is also expected to follow a universal form

$$\rho(t) \approx \kappa \left(\frac{dN}{dt}(t - T_C) \right)^{\beta} . \qquad (15)$$

The population decay rate may be due to natural effects in storage, or it could be deliberately enhanced in a controlled experiment to measure κ and β simultaneously at many locations around a ring. In this case it is perhaps more convenient to make the right hand side linear in time t by writing

$$\rho(t)^{1/\beta} \approx \kappa^{1/\beta} \frac{dN}{dt} (t - T_C) . \qquad (16)$$

The electron cloud density is expected to decay smoothly until it reaches zero and the cloud turns "off" – if the electron cloud phase transition is second order. In the following, we analyze results about this transition from experimental RHIC data and computer simulations codes (CSEC). In absence of detectors able to measure directly the linear electron density per meter, we will be focus in the study of the vacuum pressure, which can be considered as a surrogate of the electron density. Figure 4 shows the evolution of both the beam intensity (top plot) and pressure (bottom plot) for three different bunch patterns. Note that for the bunch pattern (3,12,8), when the yellow beam is injected (around 65 minutes), the lifetime of the blue beam decreases significantly, and so does the pressure. After some minutes (around 70 minutes), the pressure is already at its static value even though there is still beam on the machine, showing that the value N_c has been crossed. After a couple of minutes, the beams are aborted.

Figure 10 shows this particular case in a pressure ver-

sus beam intensity plot, which shows a second order phase transition, but suggest an exponent $\beta = 2$, according to the fit results. In order to realize how the electron cloud evolves while varying the parameter "bunch intensity", N, we run the computer simulation CSEC scanning the bunch intensity, N in small steps of $\Delta N = 0.05 \times 10^{10}$ protons from $N = 5.5$ to 6.5×10^{10} protons. The rest of the parameters are fixed to the ones in Table 1, but in this case we run 120 bunches spaced by108 ns, with no gaps since we are interested only in the saturated electron density). Figure 11 shows the computer simulation code CSEC finds is an exponent $\beta = 0.5$.

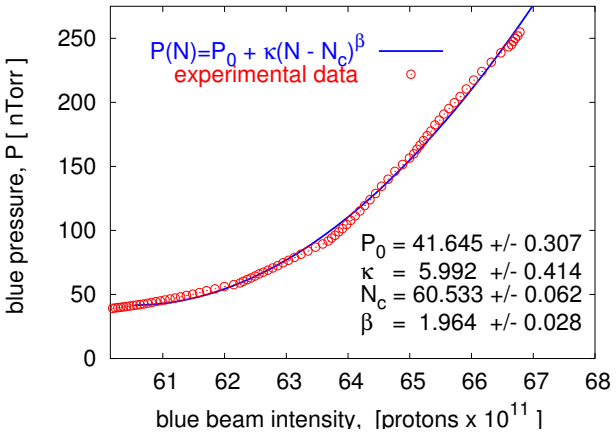

Figure 10: Experimental RHIC data showing a quadratic dependence between the pressure due to electron cloud and the total beam intensity, corresponding to the case (3,12,8) shown in Fig. 4. The curve is a fit to the data, showing an exponent $\beta = 1.964 \pm 0.026$.

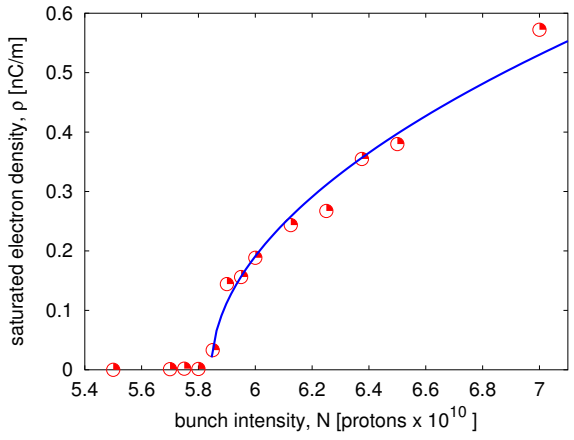

Figure 11: Simulation results using CSEC, showing a second order phase transition with a square root power law turn on. The curve is a fit to the data, with exponent $\beta = 0.509 \pm 0.017$.

RHIC data however, shows both first and second order phase transitions, as one can see in Fig. 12, which shows another example of a high intensity fill producing pressure rises in PHOBOS (IR10) and STAR (IR6). The top plot shows the pressure behaviour while the ramping process takes place: the pressure increases by about a factor of 15 in IR10, and a factor 5 in IR6. Note that the pressure in IR10 evolves much more abruptly than in IR6. Pressure in IR10 has a pronounced spike when the beams cross the transition energy, then it calms down, and it suddenly increases again when the beams go through "rebucketing", a process in which, by means of an RF gymnastics, the bunches shrink to 4 ns full parabolic bunch lenght. The bottom plot in Fig. 12 shows the evolution of the beam intensity and the bunch length while this process takes place. Finally, after about one hour, the pressure in IR10 suddenly drops, in what we can call a first order phase transition [14]. On the other hand, the pressure at IR6 evolves more adiabatically: as the bunch length decreases, the pressure smoothly increases up to a factor of 5 after the "rebucketing" and smoothly decreases as the beam intensity decreases and the bunch length increases. Note, however, that unlike the previous cases where all the discussions have been addressed for proton bunches, the case shown in Fig. 12 involves gold ion bunches, whose charge is $Z = +79$.

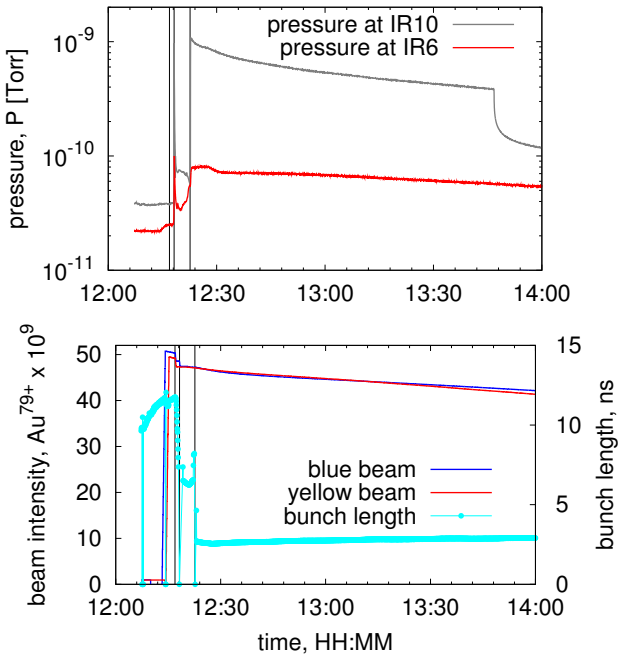

Figure 12: Pressure rise evolution at IR10, PHOBOS, and IR6, STAR, (top plot) when the ramping process starts (first vertical line, at 12:16:56), cross transition (second vertical line, at 12:18:14), and after rebucketing (at 12:22:38). The bottom plot shows the effect of these processes in the beam intensity and bunch lenght (light blue points).

Results in [20] address the situation at the Interaction Regions due to the uneven bunch spacings created by the

pass of two beams in the same chamber. The significant point to highlihgt is whether the existing electron cloud simulation codes (CSEC, ECLOUD, etc) can reproduce both the first and second order phase transitions detected at RHIC. As seen in Figures 10 and 11, whereas the experimental observations show a second order phase transition with a power exponent, $\beta \approx 2$, the exponent obtained using CSEC shows $\beta \approx 0.5$. Although experimental observations (Figures 10 and 12) shows the pressure as a function of the total beam intensity, and the computer code reproduces the electron density as a function of the bunch intensity (Fig. 11), the disagreement in the exponent between the observations and CSEC is suggesting that the computer simulation code reproducing the build up of the electron cloud do not contain all the proper physics on them.

SUMMARY AND OUTLOOK

The multi-bunch electron cloud build-up at RHIC can be determined using a third order polynomial map, written as $\vec{A} = (a, b, c)$. For a given beam pipe, these coefficients are a function of the beam parameters. The dependence of these parameters (a, b, c) on the bunch intensity, N for can be derived from electron cloud simulations codes, like CSEC or ECLOUD.

A memory of "two bunches" is found to be necessary when jumping back and forth from full to empty bunches, and therefore a complete algorithm requires four vectors: $\vec{A}_{11}$, $\vec{A}_{10}$, $\vec{A}_{00}$, and $\vec{A}_{01}$. A simulation program, MEC uses these vectors, for example to find out how to minimize the effects of the electron cloud given a machine limitation using alternative bunch patterns. Actual values for the vectors analytically demonstrate that the most sparse distribution of bunches (even when they cannot be evenly spaced) is the most stable against electron cloud effects.

In the future, and in order to obtain a better understanding of the problem, it is desirable to explore how the polynomial coefficients vary as a function of the physical parameters influencing the electron cloud (SEY, chamber dimensions, bunch spacing, bunch charge, et cetera). Application of maps to other machines (specially the B-Factories) is also interesting to study the universality of map formalism.

How the electron cloud goes from "on" to "off" is not yet an understood subject. Whereas CSEC generates a "square root" second order phase transitions, experimental observations points to a quadratic behaviour. It seems unlikely that any contemporary simulation code also reproduces first order electron cloud phase transitions, hence new physics needs to be included in the codes, in order to simulate the first order transitions routinely observed in in the PHOBOS experiment in RHIC.

ACKNOWLEDGMENTS

We are very grateful for discussions with, and support from, Mike Blaskiewicz, Angelika Drees, Wolfram Fischer, H.C. Hseuh, Nick Luciano, Giovanni Rumolo (GSI), Rogelio Tomás, Dejan Trbojevic, Lanfa Wang, and S.Y. Zhang.

REFERENCES

[1] P. Farnsworth. J. Franklin Inst, Vol. 218, Issue 4, 411-444, October 1934.

[2] G. I. Budker, G. I. Dimov, and V. G. Dudnikov, in Proceedings of the International Symposium on Electron and Positron Storage Rings,Saclay,1966 (Universitaires De France, Orsay, 1966), p. VIII-6-1.

[3] O. Gröbner, in Proceedings of the 10th International Conference on High Energy Accelerators, Serpukhov, 1977 (USSR Academy of Science, Moscow, 1977), p. 277.

[4] Review of Single-Bunch Instabilities Driven by an Electron Cloud. F. Zimmermann, Presentation at ECLOUD'04. Napa, USA, April 2004.

[5] http://wwwslap.cern.ch/collective/ecloud02/ecsim/index.html

[6] http://wwwslap.cern.ch/collective/ecloud02

[7] L. Wang, private communications.

[8] G. Rumolo, private communications.

[9] M. Blaskiewicz, private communications.

[10] Can low energy electrons affect high energy accelerators? R. Cimino, I. Collins, M. Furman, M. Pivi, G. Rumolo, F. Zimmermann. Phys. Rev. Lett. **93**, 014801 (2004).

[11] Microscopic probabilistic model for the simulation of secondary electron emission, M.A. Furman and M. Pivi, PRST-AB **5**, 124404, (2002).

[12] Electron cloud measurements and simulations for the Brookhaven Relativistic Heavy Ion Collider, W. Fischer, M. Blaskiewicz, M. Brennan, T. Satogata, PRST-AB **5**, 124401 (2002).

[13] Photoelectrons and Multipacting in the LHC : Electron Cloud Build-up, G. Stupakov, CERN-LHC-Project-Report-141, Geneva, Oct 1997.

[14] Electron cloud phase transitions, U. Iriso and S. Peggs. C-AD/AP/147, April 2004.

[15] Bunch patterns and pressure rise in RHIC, W. Fischer and U. Iriso, C-AD/AP/118, October 2003.

[16] Electron Cloud and pressure rise simulations for RHIC, U. Iriso et al, MPPE025, Proceedings of PAC'03, Portland, May 2003.

[17] RHIC Pressure Rise and Electron Cloud, S.Y. Zhang et al. MOPA010, Proceedings of PAC'03, Portland, May 2003.

[18] The Electron Cloud Effect in the Arcs of the LHC, M.A. Furman, CERN-LHC Project Report 180, Geneva, May 1998.

[19] Experimental properties of phase transitions in traffic flow, B.S. Kerner and H. Rehborn, Phys. Rev. Lett. **79** pp. 4030-33, (1997).

[20] Analysis of the electron cloud at RHIC, U. Iriso, et al. Proceedings of EPAC04, Lucern, July 2004.

Table 3: Maximum, $\rho_{\max}$, and average, ρ_{avg}, bunch to bunch values of the linear electron density computed with CSEC and MEC for two different bunch patterns. The results agree within a range of about a 15%. This error bar includes the results from analysis at Ref. [15].

parameter	unit	case no 1	case no 2	case no 3	case no 4	case no 5
bunch pattern	...	(3,68,52)	(3,23,17)	(3,12,8)	(3,4,0)(6,8,0)	(3,2,0)(6,4,0)
# of bunches	...	68	68	68	68	68
protons/bunch, N	10^{10}	8.0	8.0	8.0	8.0	8.0
$\rho_{\max}$ using CSEC	nC/m	0.8991	0.6203	0.2849	0.2221	0.2033
$\rho_{\max}$ using MEC	nC/m	0.9302	0.6645	0.2861	0.2184	0.2370
ρ_{avg} using CSEC	nC/m	0.3023	0.1433	0.0981	0.1006	0.0922
ρ_{avg} using MEC	nC/m	0.3216	0.1156	0.1045	0.0992	0.0924

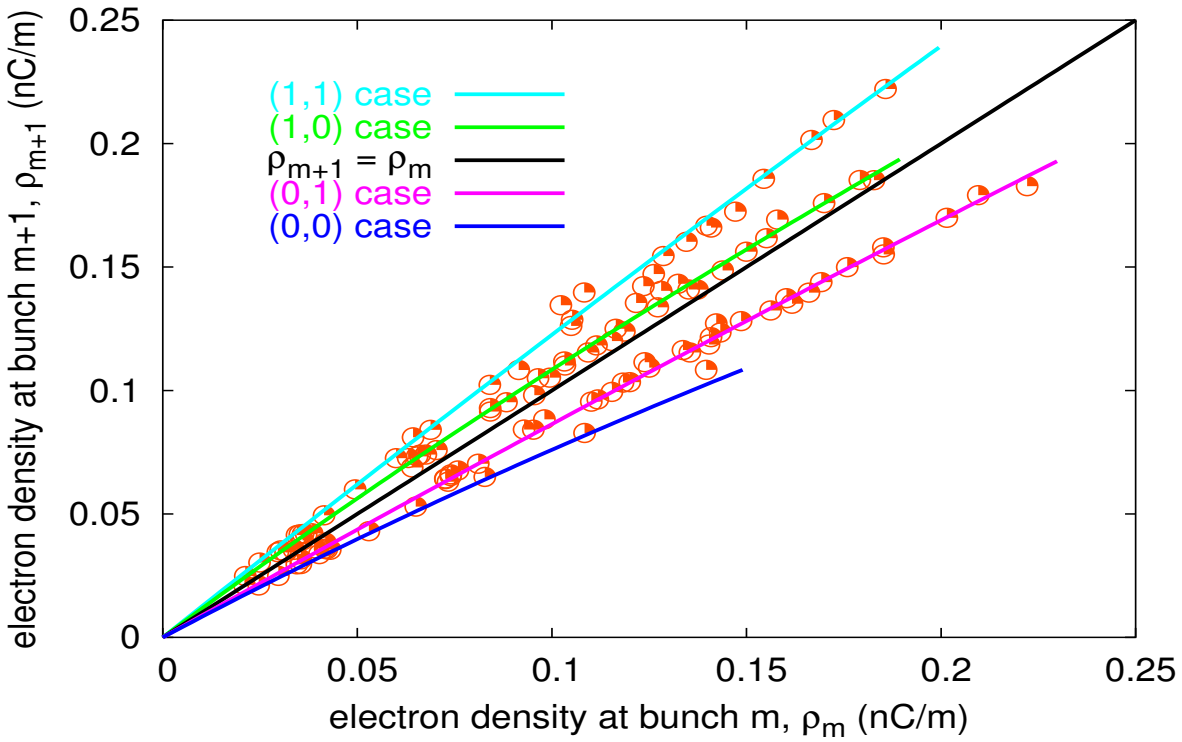

Figure 5: Electron cloud density in the (ρ_m, ρ_{m+1}) for the bunch pattern (3,4,0)(6,8,0). The plot shows that four different behaviors are required: the case (1,1) refers to "full" bunches preceded by another "full" bunch; the case (1,0) refers to "full" bunches preceded by a "phantom" bunch; the case (0,1) to "empty" bunches preceded by a "full" bunch; while the case (0,0) denotes a "phantom" bunch preceded by another "phantom" bunch.

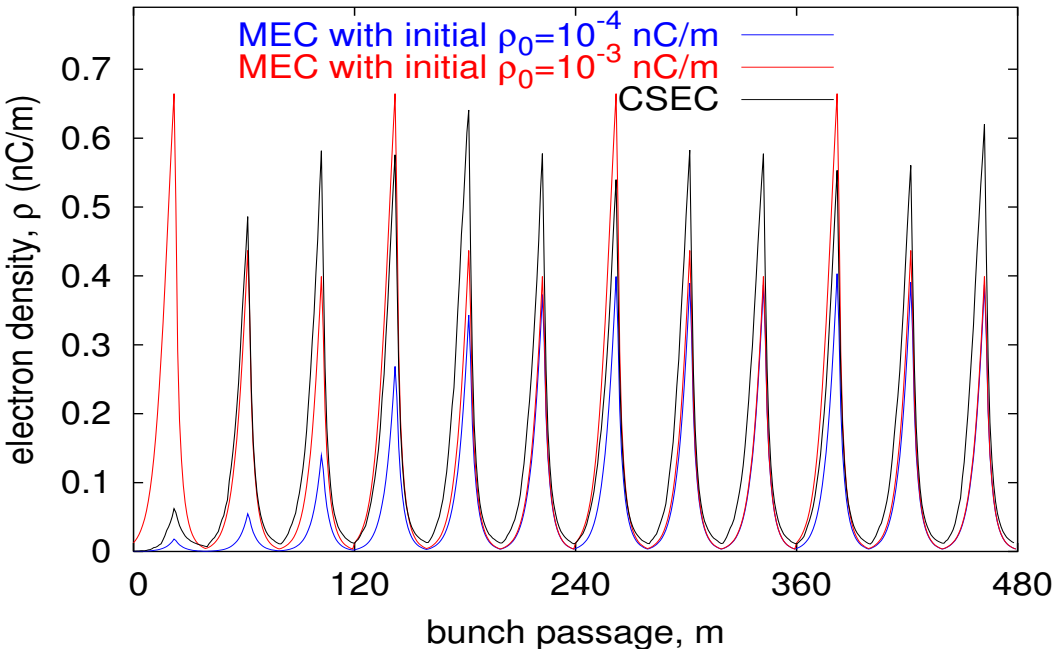

Figure 6: Electron cloud density evolution for bunch pattern (3,23.17) using CSEC (black trace) and MEC with two different initial electron densities: $\rho_0 = 10^{-4}$ nC/m (blue line) and $\rho_0 = 10^{-3}$ nC/m (red line). No matter the initial electron density, MEC results agree for the last turn (from bunch passage 360 to 480) within an acceptable error range.

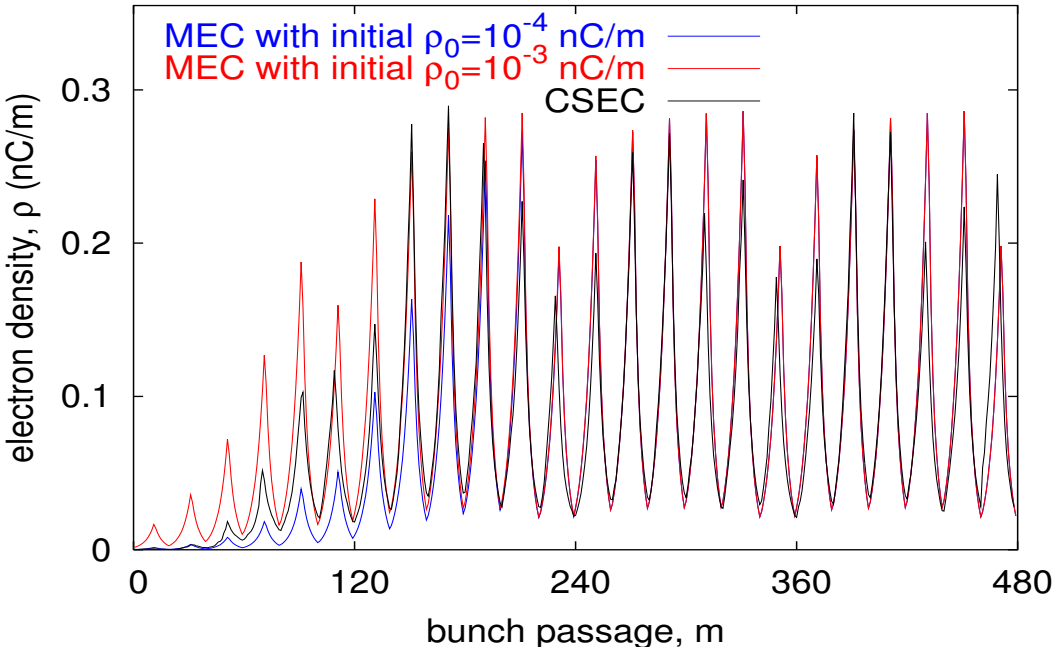

Figure 7: Electron cloud density evolution for bunch pattern (3,12,8) using CSEC (black trace) and MEC with two different initial electron densities: $\rho_0 = 10^{-4}$ nC/m (blue line) and $\rho_0 = 10^{-3}$ nC/m (red line). No matter the initial electron density, MEC results agree for the last turn (from bunch passage 360 to 480) within an acceptable error range.

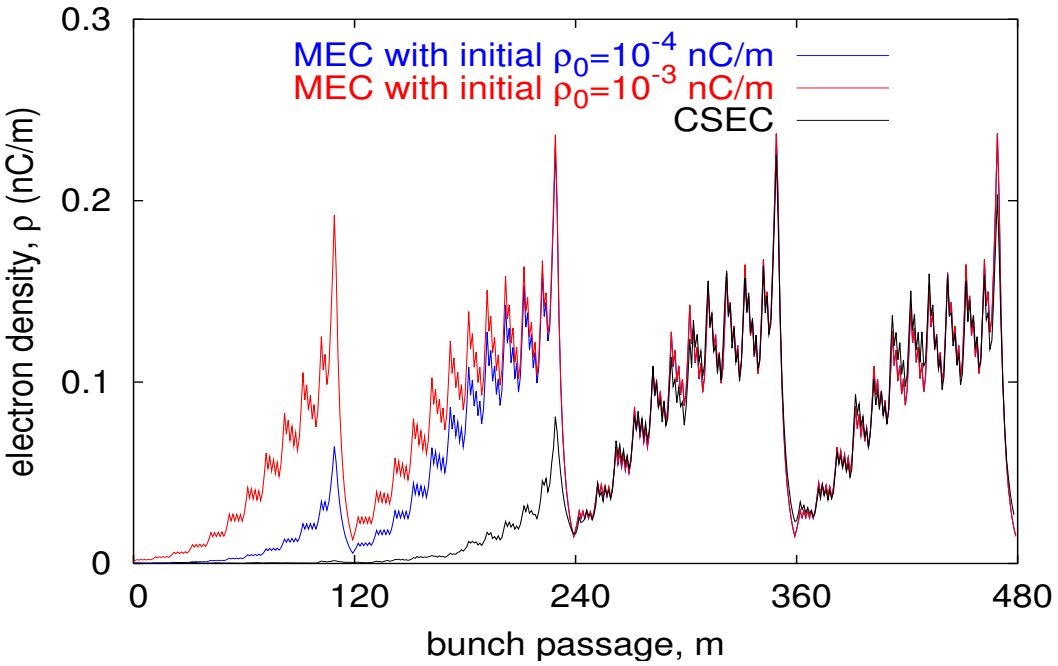

Figure 8: Electron cloud density evolution for bunch pattern (3,2,0)(6,4,0) using CSEC (black trace) and MEC with two different initial electron densities: $\rho_0 = 10^{-4}$ nC/m (blue line) and $\rho_0 = 10^{-3}$ nC/m (red line). No matter the initial electron density, MEC results agree for the last turn (from bunch passage 360 to 480) within an acceptable error range.

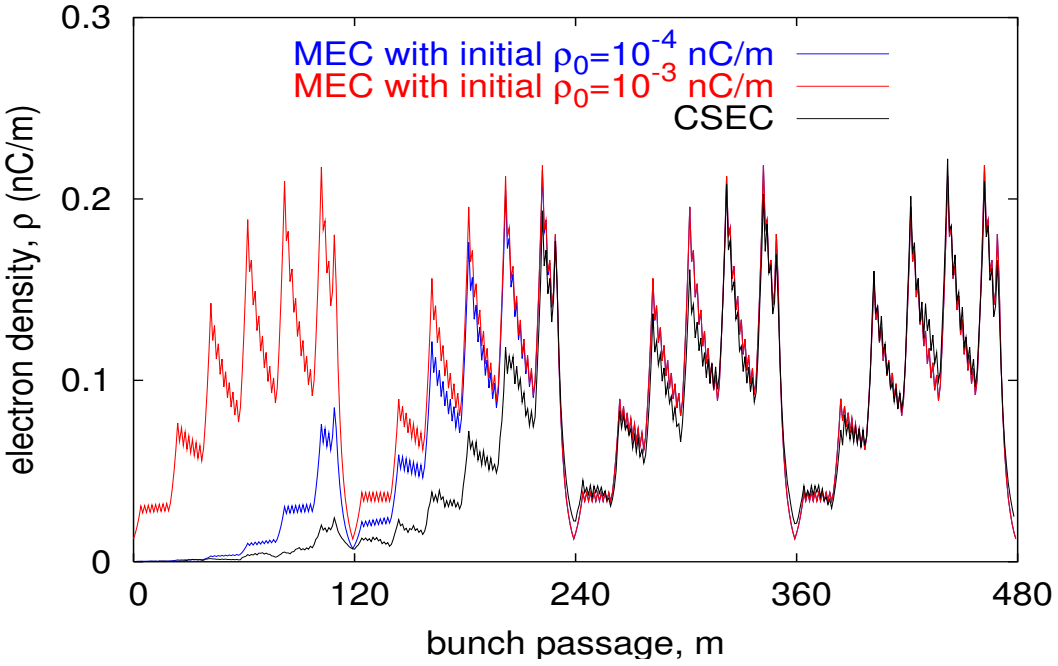

Figure 9: Electron cloud density evolution for bunch pattern (3,4,0)(6,8,0) using CSEC (black trace) and MEC with two different initial electron densities: $\rho_0 = 10^{-4}$ nC/m (blue line) and $\rho_0 = 10^{-3}$ nC/m (red line). No matter the initial electron density, MEC results agree for the last turn (from bunch passage 360 to 480) within an acceptable error range.